

Umpolung Strategy for Arene C–H Etherification Leading to Functionalized Chromanes Enabled by I(III) *N*-Ligated Hypervalent Iodine Reagents

Myriam Mikhael,^a Wentao Guo,^b Dean J. Tantillo,^{b,*} and Sarah E. Wengryniuk^{a,*}

^a Department of Chemistry, Temple University, 1901 N 13th street, Philadelphia, Pennsylvania 19122, United States
E-mail: sarahw@temple.edu

^b Department of Chemistry, University of California-Davis, 1 Shields Avenue, Davis, California 95616, United States of America
E-mail: djtantillo@ucdavis.edu

Manuscript received: June 30, 2021; Revised manuscript received: August 4, 2021;
Version of record online: ■■■, ■■■



Supporting information for this article is available on the WWW under <https://doi.org/10.1002/adsc.202100809>

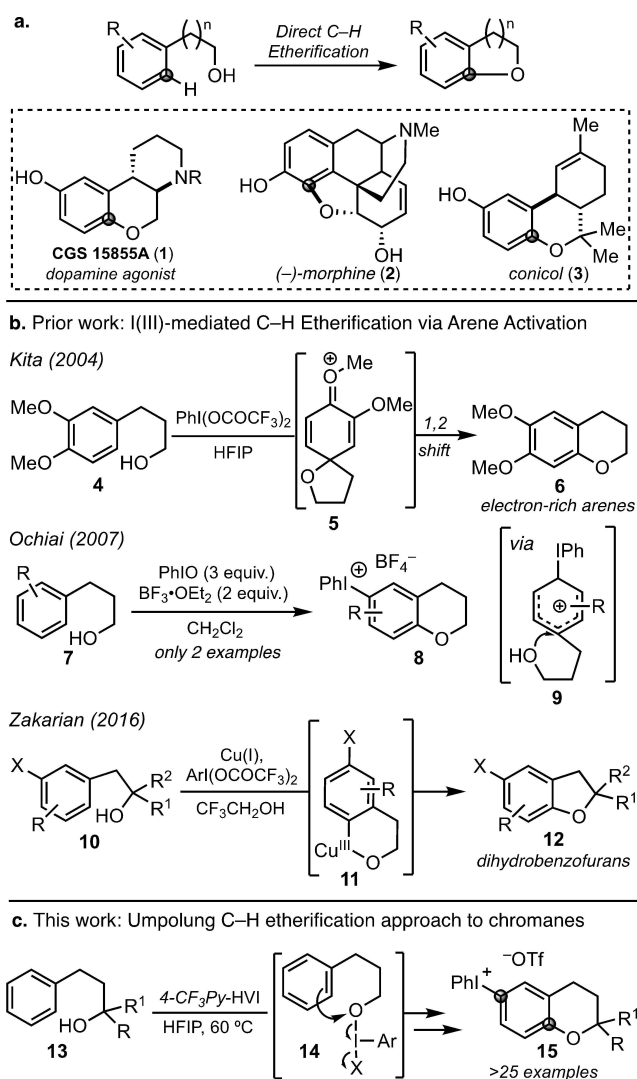
Abstract: The direct formation of aryl C–O bonds via the intramolecular dehydrogenative coupling of a C–H bond and a pendant alcohol represents a powerful synthetic transformation. Herein, we report a method for intramolecular arene C–H etherification via an umpoled alcohol cyclization mediated by an I(III) *N*-HVI reagent. This approach provides access to functionalized chromane scaffolds from primary, secondary and tertiary alcohols via a cascade cyclization-iodonium salt formation, the latter providing a versatile functional handle for downstream derivatization. Computational studies support initial formation of an umpoled O-intermediate via I(III) ligand exchange, followed by competitive direct and spirocyclization/1,2-shift pathways.

Keywords: hypervalent iodine; C–H etherification; umpolung; chromane; synthetic methods

The direct conversion of aryl C–H bonds to C–O bonds is a powerful and challenging atom- and step-economical strategy for the oxidation of aromatic rings, avoiding the pre-functionalized substrates required of traditional cross coupling manifolds (Scheme 1a).^[1] In particular, the coupling of a pendant alcohol is of high value as the resulting cyclic aryl ethers are ubiquitous scaffolds in bioactive molecules (1–3, Scheme 1a). Recent reports from the groups of Yu and Davies have demonstrated the effective use of Pd(II)/Pd(IV) for directed intramolecular aromatic C–H/C–O functionalization en route to dihydrobenzofurans,^[2] and other metals such as Cu, Fe, and Co have also shown some utility.^[3] As an

alternative to the use of expensive transition metal catalysts, hypervalent iodine (HVI) reagents have emerged as effective oxidants to achieve these transformations due to their low cost, versatile reactivity, and low toxicity.^[4] In 2004, Kita reported an intramolecular arene C–H etherification with PhI (OCOCF₃)₂ in hexafluoroisopropanol (HFIP) via the generation of an arene radical cation followed by a spirocyclization/1,2-shift to give chromanes (4 to 6, Scheme 1b).^[5] Unfortunately, yields were only moderate and the scope was limited to electron-rich arenes. In 2007, Ochiai reported a cascade sequence to give chromanyl(phenyl)λ³-iodanes (8) via cyclization on to a putative cationic intermediate (9) and subsequent electrophilic aromatic substitution from a 3-aryl-propanol (7), however scope studies were not included.^[6] Finally, a recent report from Zakarian combined I(III) arene activation with Cu(I) catalysis for the synthesis of dihydrobenzofurans via an *in situ* generated aryl iodonium salt, however the formation of larger ring sizes was prohibited, presumably as a result of the intermediacy of a Cu(III) metallocycle (11), and initial iodonium formation necessitated an activating group para to the site of functionalization.^[7]

Common to all the HVI-based approaches shown in Scheme 1 is the basic mechanism of initial arene activation and subsequent attack by the pendant alcohol. As part of our laboratory's ongoing interest in umpolung heteroatom activation with I(III) reagents,^[8] we envisioned a different approach wherein initial alcohol activation would lead to an electrophilic oxygen center (14), which could then undergo C–O bond formation via an umpoled cyclization event (Scheme 1c). It was postulated that this new reaction manifold could engage a broader substrate scope, allowing the formation of different ring sizes and overcoming the need for electron-rich aromatic rings.



Scheme 1. a. Intramolecular C–H oxidation for construction cyclic aryl ethers. b. Prior approaches using I(III) hypervalent iodine reagents c. This work: C–H etherification via umpolung oxygen cyclization with I(III) *N*-HVI.

While umpolung nitrogen activation with I(III) reagents has been demonstrated,^[4c] the corresponding oxygen activation has only been established recently.^[8a,b] Herein we report the successful application of this approach to the synthesis of functionalized chromane scaffolds via an umpolung alcohol cyclization followed by *in situ* diaryl iodonium salt formation. This process, which affects two C–H functionalizations in one pot, is enabled by a (bis)cationic nitrogen-ligated I(III) reagent (*N*-HVI)^[9] possessing two datively bound 4-*CF*₃-pyridine ligands, 4-*CF*₃-Py-HVI, which functions in both C–H functionalization events. The reaction is highly selective for cyclization over competitive alcohol oxidation and proceeds with unactivated arene rings. The resulting diaryliodonium salts provide a versatile functional handle and a

representative panel of downstream derivatizations, as well as application to the synthesis of (+/–)-conicol, are demonstrated. Experimental and computational mechanistic studies support an umpolung oxygen activation, providing the first example of this mode of reactivity for effecting C–H etherification, and provide insights into the nature of the cyclization event.

We began our investigation using 3-phenylpropanol (**16**) as a model substrate (Table 1). Of particular importance was affecting etherification over direct oxidation to the corresponding carbonyl, the latter being a competitive pathway of reported Pd-mediated C–H etherification methods^[2,10] and established reactivity with HVI reagents.^[4] Prior work from our laboratory found I(III) *N*-HVIs to be highly effective reagents for umpolung oxygen activation and capable of achieving high levels of selectivity over competitive α -elimination.^[8b] An initial screen of *N*-HVI reagents with different *N*-heterocyclic ligands, as well as traditional oxygen-ligated reagents^[11] found a marked effect on both yield and product distribution. Treatment of **16**

Table 1. Optimization of umpolung C–H etherification to chromane **17**.

R = H (**18**); 2-OMe (**19**); 4-*CF*₃ (**20**)

Entry	<i>N</i> -HVI ^[a]	Solvent ^[b]	17 : [O] ^[c]	Yield ^[d]
1	Py-HVI (18)	DCE:HFIP ^[e]	1.0:1.0	8% ^[f]
2	2-OMe-Py-HVI (19)	DCE:HFIP ^[e]	2.7:1.0	42%
3	4- <i>CF</i> ₃ -Py-HVI (20)	DCE:HFIP ^[e]	3.7:1.0	48%
4	PhI(OAc) ₂	DCE:HFIP	n.a.	0% ^[f]
5	PhI(OTFA) ₂	DCE:HFIP	17 only	14% ^[f]
6	4- <i>CF</i> ₃ -Py-HVI (20)	DCE	1.0:1.2	3% ^[f]
7	4- <i>CF</i> ₃ -Py-HVI (20)	THF:HFIP ^[e]	n.a.	trace
8	4- <i>CF</i> ₃ -Py-HVI (20)	PhH:HFIP ^[e]	3.3:1.0	47% ^[f]
9	4- <i>CF</i> ₃ -Py-HVI (20)	HFIP	17 only	66% ^[g]
10	4- <i>CF</i> ₃ -Py-HVI (20)	TFE	1.7:1.0	18% ^[f]
11	4- <i>CF</i> ₃ -Py-HVI (20) (1.1 equiv.)	HFIP	17 only	28% ^[h]
12	4- <i>CF</i> ₃ -Py-HVI (20) (2.5 equiv.)	HFIP ^[i]	17 only	73%

^[a] 2.0 equivalents of *N*-HVI were used, unless otherwise noted.

^[b] Reaction concentration 0.1 M, unless otherwise noted.

^[c] Ratio of chromane iodonium salt **17** versus direct alcohol oxidation to aldehyde. Ratios determined from ¹H NMR of crude reaction.

^[d] Isolated yield.

^[e] 1:1 (v:v) solvent ratio.

^[f] ¹H NMR yield using CH₂Br₂ as an internal standard.

^[g] Reaction run for 24 h.

^[h] Reaction run for 48 h.

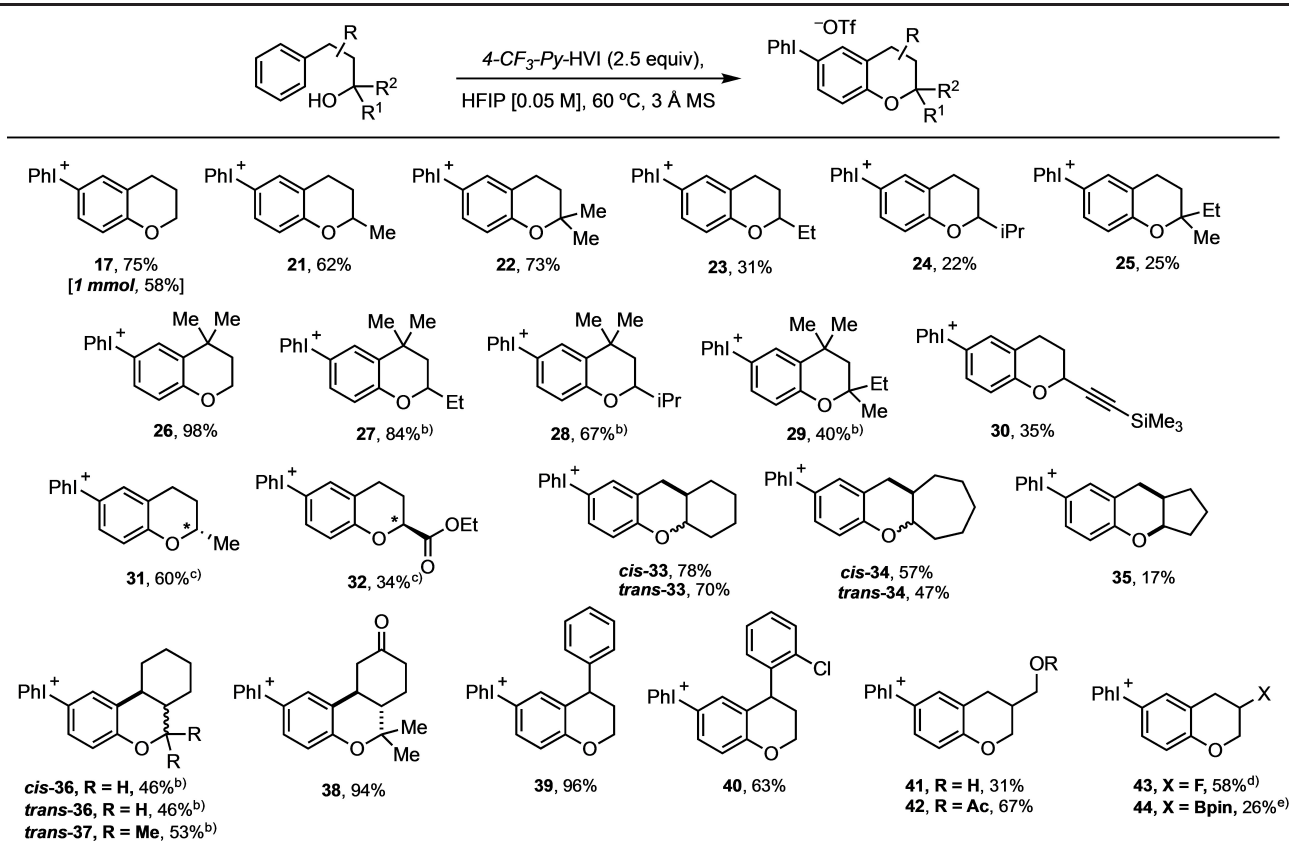
^[i] 0.05 M reaction concentration.

with 2 equivalents of *Py*-HVI (**18**) in a 1:1 mixture of DCE:HFIP at 60 °C gave just 8% conversion to chromane iodonium salt **17** and in a 1.0:1.0 ratio with aldehyde (Table 1, entry 1). Switching to 2-*OMe*-*Py*-HVI (**19**) gave a significant boost in yield to 42% with an encouraging 2.7:1.0 ratio favoring cyclization, and the electron-deficient 4-*CF*₃-*Py*-HVI (**20**) gave a slightly higher 48% yield of **17** and a further improved 3.7:1.0 ratio of cyclization to oxidation (entries 2, 3). Finally, *PhI*(OAc)₂ gave no reaction (entry 4) while *PhI*(OTFA)₂ gave selective cyclization but in very low conversion (entry 5). Further optimization was therefore conducted with 4-*CF*₃-*Py*-HVI **20**, and a solvent screen (entries 6–10) found that HFIP was essential for high conversion and selective cyclization, similar to prior reports on umpolung heteroatom activation from our laboratory.^[8a,b] Running the reaction in straight HFIP for 24 h led to a boost in yield to 66% and completely suppressed competitive aldehyde formation

(entry 9). The use of trifluoroethanol, a weaker hydrogen bond donor than HFIP, as solvent led to a significant drop in yield and selectivity (entry 10). Attempts to lower the *N*-HVI equivalents and possibly prevent subsequent iodonium formation were unsuccessful, instead giving only incomplete conversion to **17** (entry 11). Control experiments with chromane and *N*-HVI **20** confirmed that iodonium salt formation was facile under the reaction conditions (< 5 minutes). Finally, running the reaction more dilute (0.05 M) with 2.5 equiv. of 4-*CF*₃-*Py*-HVI (**20**) gave **17** in the best yield (73%) (entry 12).

With optimized conditions in hand, our attention turned to substrate scope (Table 2). We began by varying substitution at the alcohol and found that primary, secondary and tertiary alcohols all gave chromane iodonium salts in high yields (**17**, **21**–**22**), a complimentary scope to Pd-mediated etherification methods.^[2] We were surprised to find that changing the

Table 2. Alcohol Scope in umpolung C–H etherification.^[a]



^[a] Reactions run on 0.2 mmol scale. All yields are reported after isolation and purification. Reactions run for 4–6 h unless otherwise noted.

^[b] Reaction run at 23 °C.

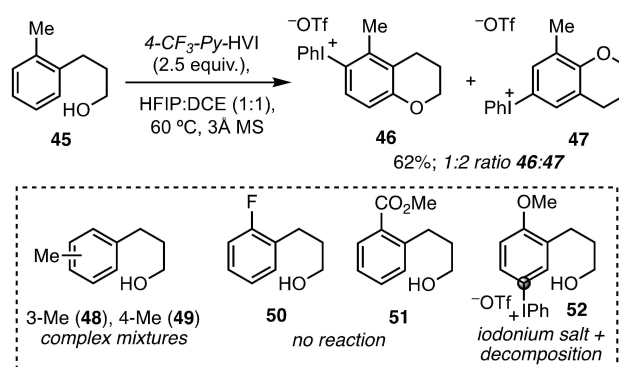
^[c] > 99:1 er. Enantiomeric ratio determined by chiral GCMS after reduction of the iodonium salt to the aryl iodide. See SI for details.

^[d] Reaction run for 24 h.

^[e] ¹H NMR yield with CH₂Br₂ as an internal standard due to issues of product instability during purification.

alcohol substituents from methyl to more substituted alkyl chains (**23–25**) led to significant drops in yield. Aldehyde byproducts were characterized in these cases, presumably arising from radical α -fragmentation, which becomes more favorable with greater substitution. Installation of a gem-dimethyl at the benzylic position overcame this issue (**26–29**), which we hypothesize to be due to enhanced rate of cyclization via the Thorpe-Ingold effect. A propargyl alcohol was cyclized to give **30** in 35% yield, hampered by competitive oxidation due to the more activated alcohol α -proton. Chiral chromanes could be synthesized from the corresponding enantioenriched alcohols with no epimerization, including 2-methyl chromane **31** in 60% yield, and ester-substituted chromane **32**, albeit in lower 34% yield due to competitive alcohol oxidation. Alcohols with both *cis* and *trans*-fused 6- and 7-membered rings cyclized in good to high yields to give tricyclic chromane scaffolds **33** and **34**, as well as **36–38**, which map on to the carbon skeleton of the cannabinoid family. In contrast, an analogous cyclopentyl alcohol cyclized to give **35** in only 17% yield, possibly due to geometric constraints preventing proper orbital overlap for cyclization. Finally, functionalization on the alkyl tether was examined. Chromanes **39** and **40** possessing a second, geminal, aromatic ring were both formed in good to excellent yield. It is noteworthy that, in the case of **39**, the second phenyl ring did not undergo iodonium salt formation, and in the case of **40**, complete chemoselectivity for cyclization onto the more electron-rich arene was observed. The presence of an additional free hydroxyl group (**41**) led to a decrease in yield, possibly due to detrimental coordination to the I(III) center, as the corresponding $-\text{OAc}$ derivative (**42**) gave a restored yield of 67%. 3-Fluorochromane (**43**) was obtained in 58% yield and an alkyl boronic ester was also tolerated, giving **44** in 26% NMR yield.

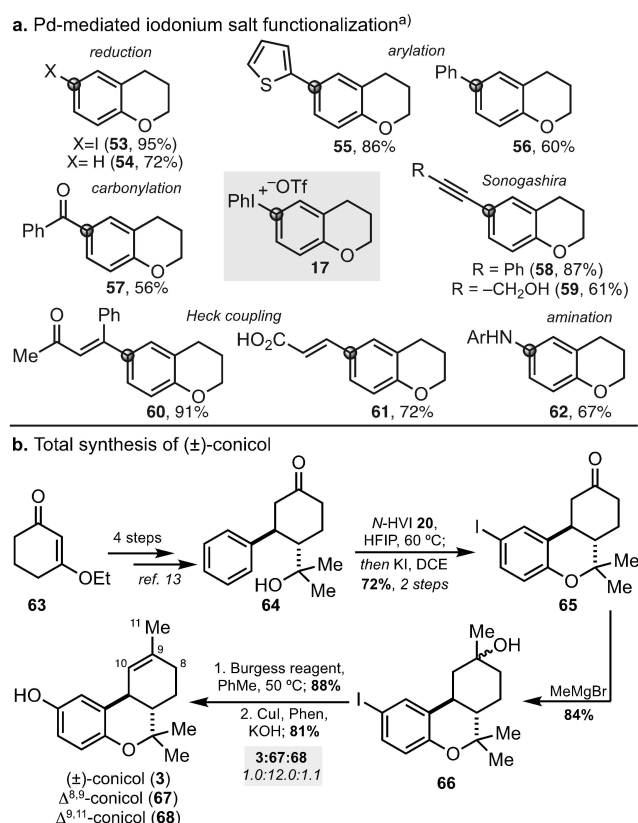
At this stage, substitution on the aromatic ring was considered (Scheme 2). We began with *o*-methyl derivative **45** and, under slightly modified conditions, obtained the desired iodonium chromane in good yield, but as a 1:2 mixture of regioisomers **46** and **47**, which could be separated via crystallization, with the major product arising from an apparent skeletal rearrangement. This result raised interesting mechanistic questions regarding the cyclization event that will be discussed subsequently. A screen of the corresponding *m*- and *p*-methyl substrates (**48**, **49**) led to complex mixtures of products. It should be noted that both **48** and **49** did produce cyclized products, however as inseparable mixtures of multiple regioisomeric chromane iodonium salts (in the case of **48**), as well as benzylic oxidation of the methyl group and other unidentified byproducts. Returning to *o*-substitution, incorporation of electron-withdrawing fluoro (**50**) or



Scheme 2. Umpolung C–H etherification with substituted arenes.

ester (**51**) substitution shut down the cyclization event, resulting in predominantly recovered starting material. Notably, introduction of an electron-donating methoxy group, which is required for prior HVI-mediated methods, led to formation of numerous byproducts including uncyclized iodonium salt **52**, highlighting the complimentary reactivity imparted by the umpolung heteroatom reaction manifold. While these results indicate that arene substitution is not broadly tolerated, this limitation is offset by the direct installation of the iodonium functional handle for downstream functionalization. Furthermore, while the formation of regioisomeric products may be detrimental to target-oriented synthesis, it would provide one-pot access to analogues for small molecule library generation.

In order to demonstrate the synthetic versatility of the obtained iodonium salts, we undertook a series of subsequent derivatizations using **17** as a model substrate (Scheme 3a). A key challenge when reacting non-symmetrical iodonium salts is selective functionalization of the arene of interest. In the case of **17**, functionalization was required on the more electron-rich arene, selectivity that is achieved primarily through the use of transition metal catalysis.^[12] After screening, it was found that Pd-catalysis was particularly effective, allowing for a broad range of transformations including reduction to the aryl iodide (**53**) or C–H (**54**), aryl- and heteroarylation (**55–56**), carbonylation (**57**), Sonogashira and Heck couplings (**58–61**), and amination (**62**). In addition, the synthetic utility of the approach was demonstrated through a concise total synthesis of (+/–)-conicol (Scheme 3b). The key cyclization proceeded smoothly from ketone **64** followed by reduction to the aryl iodide to give **65** in 72% over two steps. Iodochromane **65** could then be advanced to (+/–)-conicol (**3**) in just three additional steps; late-stage installation of the A-ring olefin from **66** gave a mixture of three double bond isomers, desired (+/–)-conicol (**3**), along with $\Delta^{8,9}$ -conicol (**67**) and $\Delta^{9,11}$ -conicol (**68**), in a 1.0:11.2:1.1 ratio. This



Scheme 3. a. Downstream functionalization of chromane iodonium salt. b. Application to the total synthesis of (+/–)-conicol. a) See Supporting Information for procedures for conversion of **17** to **53–62**.

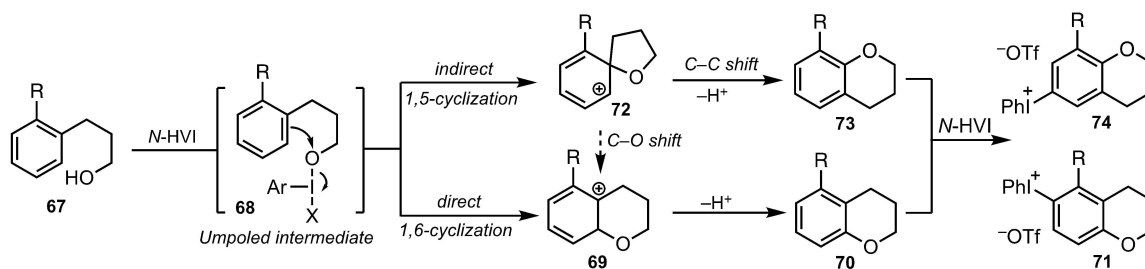
result provides insights into the innate reactivity of the cannabinoid scaffolds and viability of late-stage double bond installation en route to these molecules.

Finally, the mechanism of the proposed umpolung cyclization event and subsequent arene functionalization was examined, both through experiment and computation. Computational studies were performed using density functional theory (DFT) calculations with *Gaussian16 C.01*.^[14] The M06-2X hybrid functional was used, given precedent for its effectiveness in treating halogen bonds.^[15] Specifically, we

employed the M06-2X-D3(0) method with a mixed basis set containing 6-31G(d) for C, N, O and H, and SDD for I.^[16] The HFIP/DCE solvent mixture used experimentally was approximated using trifluoroethanol modeled with the SMD continuum solvation model.^[17] Single point energies of competing transition state structures (TSSs) also were computed using two sets of adapted parameters for HFIP and no significant changes were observed (see SI for details).^[18] Conformational searching was performed with XTB-CREST.^[19]

Based on prior findings in our laboratory, we proposed an initial ligand exchange between the alcohol and *N*-HVI to give key umpoled intermediate **68** (Scheme 4).^[8a,b] The formation of regioisomeric cyclization products when using a substituted arene (see Scheme 2) then led us to two possible cyclization modes. A direct 1,6-cyclization would give **69**, followed by rearomatization and iodonium salt formation with a second equivalent of *N*-HVI to give chromane **71**. Alternatively, a 1,5-spirocyclization would give **72**, which could either undergo a 1,2-C–O shift to converge on intermediate **69**, or a 1,2-C–C shift to form rearranged product **73** and then **74** after subsequent functionalization.

Beginning with formation of an umpoled intermediate such as **68**, a control experiment from the corresponding methyl ether of **16**, which would not undergo ligand exchange with the I(III) reagent, gave exclusively unreacted starting material under our standard conditions, indicating that initial arene activation, as proposed by Ochiai, was not operative (see Supporting Information). Ochiai's mechanism was also probed computationally, however a minimum for an intermediate with arene bound to 4-*CF*₃-Py-HVI could not be located (see Supporting Information). Furthermore, NMR analysis of a 1:1 mixture of **16** with *N*-HVI **20** in CDCl₃ revealed rapid (<5 min) formation of a new species, with downfield shifts of the methylene alpha to the oxygen center (see Supporting Information). This spectral data aligned well with a prior study from Togo and Yokoyama on the ligation of **16** with PhI(OAc)₂.^[20] Computational studies on **68** (R=H) found four low energy conformers, with the



Scheme 4. Proposed mechanism of umpolung C–H etherification.

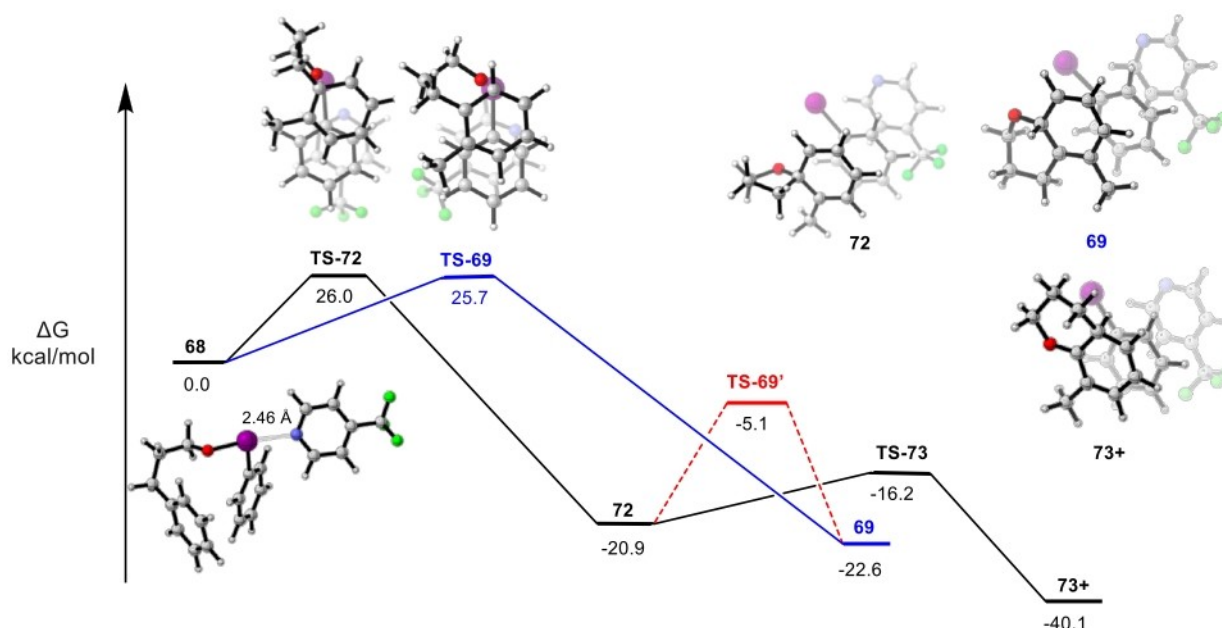


Figure 1. Free energy profile of reaction pathway from **68** to **69** and **73+** (protonated form of **73**), along with CYLview images of structures [CYLview, 1.0b; Legault, C. Y., Université de Sherbrooke, 2009 (<http://www.cylview.org>)]. Relative free energies shown are for stationary points optimized in trifluoroethanol using a SMD continuum solvation model at the M06-2X-D3(0)/6-31 g(d) + SDD level of theory. Only the TSSs with the lowest energy are shown above. See Supporting Information for the discussion of TSSs conformations and energies in different solvation.

lowest energy structure having an I–N bond length of 2.46 Å between the nitrogen of CF₃-pyridine and the iodonium iodine (Figure 1). ¹³C and ¹H NMR chemical shifts were also computed for the four conformers,^[21] and the computed shifts of the lowest energy conformer match well with the aforementioned experimental shifts (see Supporting Information), providing confidence in both the structural assignment and the computational approach.

Next, the significance of the I(III) reagent in umpolung oxygen activation was probed computationally as a clear effect of the X-ligand on the efficiency of cyclization was observed in initial screening (see Table 1). To begin, two parameters regarding the ligated I–O intermediate (**68**) were studied. Using three different schemes to calculate atomic charge, the relative atomic charge on oxygen with various X-ligands (Table 3) was examined and showed a trend consistent with experimental results. The use of 4-CF₃-Py-HVI (**20**), Py-HVI (**18**) and PhI(OTFA)₂ gave comparable levels of negative charge on oxygen and all were capable of promoting some degree of cyclization, whereas PhI(OAc)₂ gave significantly higher values and was unreactive. Next, the relative LUMO energies of the complexed intermediates were examined (Table 4). Interestingly, while all had significant I–O σ* character, the two *N*-HVI reagents resulted in dramatically lower LUMO energies relative to the two O-ligated complexes, potentially indicating the

Table 3. Oxygen centered atomic charge of **68** analogs with varied X-ligands.

Atomic Charge	68 -[PhI(4-CF ₃ -Py) ₂] 2OTf	68 -[PhI(Py) ₂] 2OTf	68 -PhI(OTFA) ₂	68 -PhI(OAc) ₂
CHELPG ^[a]	−0.44	−0.49	−0.48	−0.69
RESP ^[b]	−0.38	−0.45	−0.40	−0.61
MK ^[c]	−0.38	−0.46	−0.40	−0.61

^[a] CHELPG: charges from electrostatic potentials using a Grid-based method.^[22]

^[b] RESP: restrained electrostatic potential atomic partial charges.^[23] and

^[c] MK: Merz-Singh-Kollman (MK) Scheme.^[24] Results are given by wavefunction analysis software Multiwfn.^[25]

Table 4. Calculated LUMOs for **68** analogs with varied X-ligands using NBO analysis.

68 Analog	LUMO Energy (eV) ^[a]
68 -[PhI(4-CF ₃ -Py) ₂] 2OTf	−4.6 eV
68 -[PhI(Py) ₂] 2OTf	−3.4 eV
68 -PhI(OTFA) ₂	−0.4 eV
68 -PhI(OAc) ₂	−0.4 eV

Energies are given by NBO calculations with M06-2x-D3(0)/6-31 g(d) + SDD(I).

significance of *N*-HVI reagents in promoting umpolung heteroatom activation.

From O-ligated **68**, computational studies were performed on the three subsequent stages en route to either **71** or **74** ($R=CH_3$): I) C–O cyclization, which may be direct or indirect; II) 1,2-shift of either a C- or O-based migrating group; and III) deprotonation followed by electrophilic aromatic substitution of the resulting chromane. For Stage I, we predict that both direct formation of protonated chroman **69** and indirect formation via spiro compound **72** are possible. The relative free energies of the competing cyclization TSSs, **TS-69** and **TS-72**, are very close to each other, as shown in Figure 1 (see SI for a discussion of TSS conformations), consistent with the low **46:47** selectivity observed experimentally (Scheme 2), assuming that **72** strongly prefers to form **73** over **69** (*vide infra*). To further probe the role of I(III) X-ligand in the umpolung cyclization, the transition state energies for **TS-69** and **TS-72** were also examined from activation with $PhI(OTFA)_2$ and $PhI(OAc)_2$ and found to be 2.2 and 0.2 kcal/mol higher, respectively, for $PhI(OTFA)_2$ and 15.5 and 6.9 kcal/mol higher for $PhI(OAc)_2$, again consistent with experimental observations that these reagents were significantly less effective at promoting cyclization (see Supporting Information). For Stage II, prior work from Ochiai^[6] and McClelland^[26] predicted that C–C bond migration was favored by ~6 kcal/mol (B3LYP/6-31G*) over C–O bond migration. Our calculations aligned with these findings, with a free energy barrier for the C–C shift of **72** that is 11.1 kcal/mol lower than that for C–O shift, indicating that the selectivity of **46:47** is reflective of the ratio of direct (forming **69**) vs indirect (forming **72**) cyclization events.^[27] For Stage III, we attempted but failed to locate TSSs for electrophilic aromatic substitution (EAS). Whether or not discrete TSSs for EAS reactions can be located is system-dependent and also intimately tied to the treatment of solvent (e.g., modeling explicit solvent here was not feasible, especially given that a solvent mixture was used).^[28] Not surprisingly, attack at the position para to the R-group is favored for $R=OCH_3$ based on computed proton affinities, consistent with the experimental observation of uncyclized iodonium salt **52** (Scheme 2). Step III was also probed experimentally

wherein unsubstituted chromane (**67**, $R=H$) was subjected to slightly modified reaction conditions and rapid conversion to iodonium salt **17** was observed (see Supporting Information). We also considered the possibility of pathways involving O-centered radicals, but these do not appear to be energetically viable (see Supporting Information).

Reactions involving competing additions to two adjacent positions sometimes involve post-transition bifurcations,^[29] so we considered that possibility here for **68**→**69**+**72**. In such a scenario, one or both of the cyclization TSSs would lead to both products through pathways that decrease monotonically in energy. This phenomenon can be probed using quasi-classical ab initio molecular dynamics (AIMD) simulations (carried out here using Singleton's Progdyn).^[30] We chose two transition state conformations for each of **TS-69** and **TS-72** and collected ~50 trajectories for each (Table 5). For each transition state, both products were indeed found, although only ~2% of the trajectories for each transition state led to the product expected for the competing transition state. While recognition that the transition states are followed by bifurcations does not change our selectivity predictions in this case, it may well in other related cases.^[31]

In conclusion, we report the synthesis of functionalized chromane scaffolds via a dual C–H functionalization cascade initiated by an umpoled oxygen cyclization event. The reaction is mediated by an I(III) *N*-HVI, 4- CF_3 -Py-HVI, which was required for high reactivity as well as high selectivity for cyclization over competitive oxidation. The activation strategy allows for use of electronically-neutral arenes and is compatible with primary, secondary, and tertiary alcohols, complimenting existing HVI and metal-catalyzed methodologies. The one-pot installation of an iodonium salt functional handle allows for diverse and selective downstream manipulations. Finally, experimental and computational studies support the formation of an umpoled oxygen intermediate as well as competitive direct and spirocyclization pathways for the key C–O bond forming event. Further studies on the application of this platform to other umpolung C–H functionalizations are currently underway in our laboratory and will be reported in due course.

Table 5. Results of quasi-classical molecular dynamics simulations for trajectories initiated from each of the two conformations of **TS-69** and **TS-72**.

	Conformation	68–68 (SM–SM recrossing)	68–72 (1,5-cyclization)	68–69 (1,6-cyclization)	Total trajectories
TS-69	boat	2	1	43	46
TS-69	chair	3	1	46	50
TS-72	1	1	44	0	45
TS-72	2	0	45	1	47

Experimental Section

General Procedure for *N*-HVI Umpolung C–H Etherification. Alcohol (0.2 mmol, 1.0 equiv.) was added to a flame dried test tube under argon equipped with activated 3 Å MS, followed by distilled HFIP (2.0 mL, 0.1 M). *N*-HVI (0.5 mmol, 2.5 equiv.) dissolved in 2.0 mL of dry HFIP was then added to the reaction flask under argon and the mixture was heated to the desired temperature. Reaction was followed by TLC. Upon completion, mixture was concentrated *in vacuo* and HFIP was completely removed by azeotrope with CH₂Cl₂. Concentrated mixture was then diluted in CH₂Cl₂ and washed with 1.0 mL of H₂O. Aqueous layer was back extracted with CH₂Cl₂ (×2), and the combined organic layers were dried over Na₂SO₄, filtered, and concentrated *in vacuo*. Crude reaction was purified by flash chromatography through solid loading (more details in Supporting Information) and eluted using a solvent gradient as indicated with each substrate.

Acknowledgements

The authors are grateful to the National Science Foundation (NSF CAREER 152244 and CHE-1856416) and National Institutes of Health (NIH R01 GM123098) for financial support of this work. The authors thank Dr. Charles DeBrosse (Temple University) for NMR spectroscopic assistance and Dr. Charles W. Ross III, Director: Automated Synthesis and Characterization at University of Pennsylvania Chemistry for providing high-resolution mass spectral data. The authors would also like to acknowledge the Telluride Science Research Center meeting on Accelerating Reaction Discovery (2020) that prompted the collaboration described herein.

References

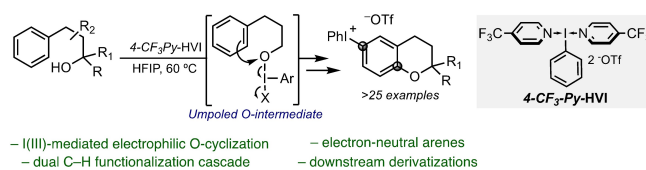
- [1] a) T. W. Lyons, M. S. Sanford, *Chem. Rev.* **2010**, *110*, 1147–1169; b) B. Liu, B.-F. Shi, *Tetrahedron Lett.* **2015**, *56*, 15–22; c) C. Yuan, Y. Liang, T. Hernandez, A. Berriochoa, K. N. Houk, D. Siegel, *Nature* **2013**, *499*, 192–196.
- [2] a) X. Wang, Y. Lu, H.-X. Dai, J.-Q. Yu, *J. Am. Chem. Soc.* **2010**, *132*, 12203–12205; b) H. Wang, G. Li, K. M. Engle, J.-Q. Yu, H. M. L. Davies, *J. Am. Chem. Soc.* **2013**, *135*, 6774–6777.
- [3] For the synthesis of related scaffolds such as dibenzofurans, benzofuranones, and biaryllactones via metal-catalyzed intramolecular C–H/C–O bond formation see: P. J. Borpatra, B. Deka, M. L. Deb, P. K. Baruah, *Org. Chem. Front.* **2019**, *6*, 3445–3489.
- [4] a) *Hypervalent Iodine Chemistry*; T. Wirth, Ed.; Springer: Switzerland, 2016; b) V. V. Zhdankin, P. J. Stang, *Chem. Rev.* **2008**, *108*, 5299–5358; c) A. Yoshimura, V. V. Zhdankin, *Chem. Rev.* **2016**, *116*, 3328–3435.
- [5] a) H. Hamamoto, K. Hata, H. Nambu, Y. Shiozaki, H. Tohma, Y. Kita, *Tetrahedron Lett.* **2004**, *45*, 2293–2295; b) K. Hata, H. Hamamoto, Y. Shiozaki, S. B. Cammerer, Y. Kita, *Tetrahedron Lett.* **2007**, *63*, 4052–4060.
- [6] K. Miyamoto, M. Hirobe, M. Saito, M. Shiro, M. Ochiai, *Org. Lett.* **2007**, *9*, 1995–1998.
- [7] J. Alvarado, J. Fournier, A. Zakarian, *Angew. Chem. Int. Ed. Engl.* **2016**, *55*, 11625–11628.
- [8] a) B. T. Kelley, J. C. Walters, S. E. Wengryniuk, *Org. Lett.* **2016**, *18*, 1896–1899; b) J. C. Walters, A. F. Tierno, A. H. Dubin, S. E. Wengryniuk, *Eur. J. Org. Chem.* **2018**, 1460–1464; c) M. Mikhael, S. Adler, S. E. Wengryniuk, *Org. Lett.* **2019**, *21*, 5889–5893.
- [9] a) R. Weiss, J. Seubert, *Angew. Chem. Int. Ed. Engl.* **1994**, *33*, 891–893; b) R. Corbo, J. L. Dutton, *Coord. Chem. Rev.* **2018**, *375*, 69–79.
- [10] a) K. E. Torraca, S.-I. Kuwabe, S. L. Buchwald, *J. Am. Chem. Soc.* **2000**, *122*, 12907–12908; b) A. V. Vorogushin, X. Huang, S. L. Buchwald, *J. Am. Chem. Soc.* **2005**, *127*, 8146–8149.
- [11] For full screening details, see Supporting Information.
- [12] a) E. A. Merritt, B. Olofsson, *Angew. Chem. Int. Ed. Engl.* **2009**, *48*, 9052–9070; b) B. Olofsson, *Top. Curr. Chem.* **2016**, *27*, 1456; c) D. R. Stuart, *Chem. Eur. J.* **2017**, *23*, 15852–15863.
- [13] A. D. William, Y. Kobayashi, *J. Org. Chem.* **2002**, *67*, 8771–8782.
- [14] Gaussian 16, Revision C.01, M. J. Frisch, G. W. Trucks, H. B. Schlegel, G. E. Scuseria, M. A. Robb, J. R. Cheeseman, G. Scalmani, V. Barone, G. A. Petersson, H. Nakatsuji, X. Li, M. Caricato, A. V. Marenich, J. Bloino, B. G. Janesko, R. Gomperts, B. Mennucci, H. P. Hratchian, J. V. Ortiz, A. F. Izmaylov, J. L. Sonnenberg, D. Williams-Young, F. Ding, F. Lipparini, F. Egidi, J. Goings, B. Peng, A. Petrone, T. Henderson, D. Ranasinghe, V. G. Zakrzewski, J. Gao, N. Rega, G. Zheng, W. Liang, M. Hada, M. Ehara, K. Toyota, R. Fukuda, J. Hasegawa, M. Ishida, T. Nakajima, Y. Honda, O. Kitao, H. Nakai, T. Vreven, K. Throssell, J. A. Montgomery, Jr., J. E. Peralta, F. Ogliaro, M. J. Bearpark, J. J. Heyd, E. N. Brothers, K. N. Kudin, V. N. Staroverov, T. A. Keith, R. Kobayashi, J. Normand, K. Raghavachari, A. P. Rendell, J. C. Burant, S. S. Iyengar, J. Tomasi, M. Cossi, J. M. Millam, M. Klene, C. Adamo, R. Cammi, J. W. Ochterski, R. L. Martin, K. Morokuma, O. Farkas, J. B. Foresman, D. J. Fox, Gaussian, Inc., Wallingford CT, 2016.
- [15] a) M. Walker, A. J. A. Harvey, A. Sen, C. E. H. Dessent, *J. Phys. Chem. A* **2013**, *117*, 12590–12600; b) S. Kouch, J. M. L. Martin, *J. Chem. Theory Comput.* **2013**, *9*, 1918–1931.
- [16] a) S. Grimme, *Wiley Interdiscip. Rev.: Comput. Mol. Sci.* **2011**, *1*, 211–228; b) P. C. Hariharan, J. A. Pople, *Theor. Chim. Acta* **1973**, *28*, 213–222; c) G. Igel-Mann, H. Stoll, H. Preuss, *Mol. Phys.* **1988**, *65*, 1321–1328.
- [17] A. V. Marenich, C. J. Cramer, D. G. Truhlar, *J. Phys. Chem. B* **2009**, *113*, 6378–6396.
- [18] a) E. Richmond, J. Yi, V. D. Vukovic, F. Sajadi, C. N. Rowley, J. Moran, *Chem. Sci.* **2018**, *9*, 6411–6416; b) A. A. Hussein, Y. Ma, A. Al-Yasari, *Eur. J. Org. Chem.* **2020**, 7219–7228.
- [19] S. Grimme, *J. Chem. Theory Comput.* **2019**, *15*, 2847–2862.


- [20] H. Togo, T. Muraki, Y. Hoshina, K. Yamaguchi, M. Yokoyama, *J. Chem. Soc. Perkin Trans. 1* **1997**, 787–794.
- [21] a) D. Sethio, G. Raggi, R. Lindh, M. Erdelyi, *J. Chem. Theory Comput.* **2020**, *16*, 7690–7701; b) J. R. Cheeseman, G. W. Trucks, T. A. Keith, M. J. Frisch, *J. Chem. Phys.* **1996**, *104*, 5497–5509; c) A. G. Kutateladze, D. S. Reddy, *J. Org. Chem.* **2017**, *82*, 3368–3381.
- [22] C. M. Breneman, K. B. Wiberg, *J. Comput. Chem.* **1990**, *11*, 361–373.
- [23] C. I. Bayly, P. Cieplak, W. D. Cornell, P. A. Kollman, *J. Phys. Chem.* **1993**, *97*, 10269–10280.
- [24] U. C. Singh, P. A. Kollman, *J. Comput. Chem.* **1984**, *5*, 129–145.
- [25] T. Lu, F. Chen, *J. Comput. Chem.* **2012**, *33*, 580–592.
- [26] a) A. Goosen, C. W. McClelland, F. B. Rinaldi, *J. Chem. Soc. Perkin Trans. 2* **1993**, 279–281; b) C. McClelland, G. D. Ruggiero, I. H. Williams, *J. Chem. Soc. Perkin Trans. 2* **2002**, 204–208.
- [27] The difference in origin of **46** in our work versus Ochiai's (1,6-direct cyclization vs C–O bond shift) is reflected in a difference in ratio of **46:47**. Ochiai reported a ratio of **46:47** of 1.0:3.3, relative our finding of 1.0:2.0. Ochiai's work did not include a direct cyclization pathway to access **46**, thus resulting in the lower ratio of the non-rearranged product (**46**).
- [28] Y. Nieves-Quinones, D. A. Singleton, *J. Am. Chem. Soc.* **2016**, *138*, 15167–15176.
- [29] a) D. H. Ess, S. E. Wheeler, R. G. Iafe, L. Xu, N. Celebi-Olcum, K. N. Houk, *Angew. Chem. Int. Ed.* **2008**, *47*, 7592–7601; *Angew. Chem.* **2008**, *120*, 7704–7713; b) S. R. Hare, D. J. Tantillo, *Pure Appl. Chem.* **2017**, *89*, 679–698.
- [30] a) X. Ma, W. L. Hase, *Phil. Trans. R. Soc. A* **2017**, *375*, 1–20; b) Z. Chen, Y. Nieves-Quinones, J. R. Waas, D. A. Singleton, *J. Am. Chem. Soc.* **2014**, *136*, 13122–13125.
- [31] S. R. Hare, A. Li, D. J. Tantillo, *Chem. Sci.* **2018**, *9*, 8937–8945.

COMMUNICATIONS

Umpolung Strategy for Arene C–H Etherification Leading to Functionalized Chromanes Enabled by I(III) *N*-Ligated Hypervalent Iodine Reagents

Adv. Synth. Catal. **2021**, 363, 1–10



 M. Mikhael, W. Guo, Prof. Dr. D. J. Tantillo*, Prof. Dr. S. E. Wengryniuk*